THE JOURNAL OF PHYSICAL CHEMISTRY B

Article

pubs.acs.org/JPCB

Conductance, a Contrivance To Explore Ion Association and Solvation Behavior of an Ionic Liquid (Tetrabutylphosphonium Tetrafluoroborate) in Acetonitrile, Tetrahydrofuran, 1,3-Dioxolane, and Their Binaries

Deepak Ekka and Mahendra Nath Roy*

Department of Chemistry, University of North Bengal, Darjeeling 734 013, India

ABSTRACT: Precise measurements on electrical conductance (Λ) of solutions of an ionic liquid (IL) tetrabutylphosphonium tetrafluoroborate in acetonitrile (ACN), tetrahydrofuran (THF), and 1,3-dioxolane (1,3-DO) and their binary mixtures have been reported at 298.15 K. The conductance data have been analyzed by the Fuoss conductance equation (1978) in terms of the limiting molar conductance (Λ_o), the association constant (K_A), and the association diameter (R) for ion-pair formation. The Walden product is obtained and discussed. However, the deviation of the conductometric curves (Λ versus $\sqrt{c}$) from linearity for the electrolyte in THF and 1,3-DO and their binary mixtures indicated triple-ion formation and therefore the corresponding conductance data have been analyzed by the Fuoss–Kraus theory of triple ions. The limiting ionic conductances ($\lambda_o^{\pm}$) have been estimated from the appropriate division of the limiting molar conductivity value of tetrabutylammonium tetraphenylborate [Bu_4NBPh_4] as the "reference electrolyte" method along with a numerical evaluation of ion-pair and triple-ion formation constants ($K_P \approx K_A$ and K_T). The results have been discussed in terms of solvent properties and configurational theory. Ionic association in the limiting molar conductances as well as the single-ion conductivity values have been determined for the electrolyte in the solvent media.

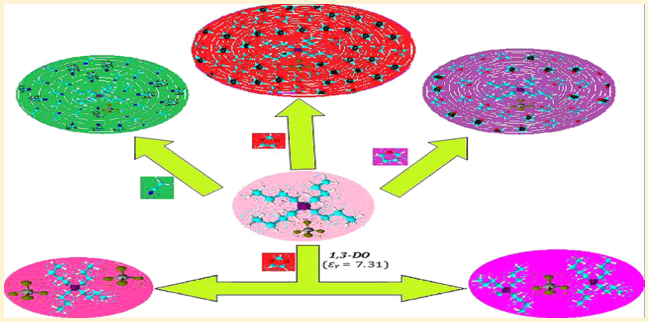

1. INTRODUCTION

In recent years, ionic liquids (ILs) have been considered attractive compounds due to their unique intrinsic properties, such as negligible vapor pressure, large liquid range, ability of dissolving a variety of chemicals, high thermal stability, and large electrochemical window and their potential as "designer solvents" and "green" replacements for volatile organic solvents[1−3] used in reactions involving inorganic and biocatalysis, etc. They are also used as heat-transfer fluids for processing biomass and as electrically conductive liquids in electrochemistry (batteries and solar cells).[4−6] In modern technology, the application of the salt is well understood by studying the ionic solvation or ion association.

Consequently, a number of conductometric[7] and related studies of electrolytes in nonaqueous solvents, especially mixed organic solvents, have been made for their optimal use in high-energy batteries[8] and for further understanding organic reaction mechanisms.[9] Ionic association of electrolytes in solution depends upon the mode of solvation of its ions[10−13] which in turn depends on the nature of the solvent/solvent mixtures. Such solvent properties as viscosity and the relative permittivity have been taken into consideration as these properties help in determining the extent of ion association and the solvent−solvent interactions. The nonaqueous system has been of immense importance[14,15] to the technologist and theoretician as many chemical processes occur in these systems. Thus, extensive studies on electrical conductance in various mixed organic solvents have been performed in recent years[16−20] to examine the nature and magnitude of ion−ion and ion−solvent interactions.

In continuation of our investigations on electrical conductance,[17,18,21] an attempt has been made in the present study to ascertain the nature of ion−solvent interactions of ionic liquid (IL) tetrabutylphosphonium tetrafluoroborate [Bu_4PBF_4] in polar aprotic solvents pure acetonitrile, tetrahydrofuran, 1,3-dioxolane, and their binary mixtures, as literature survey reveals that very little work has been carried out with the binary mixtures.

2. EXPERIMENTAL SECTION

2.1. Source and Purity of Samples. [Bu_4PBF_4] of puriss grade was procured from Sigma-Aldrich, Germany and was used as purchased. The mass fraction purity of [Bu_4PBF_4] was ≥0.99.

Acetonitrile (ACN) obtained from Merck, India, was used after further purification. It was distilled from P_2O_5 and then from CaH_2 in an all-glass distillation apparatus.[22] The middle fraction was collected. About 99% purified acetonitrile with

Received: March 14, 2012
Revised: July 24, 2012
Published: August 31, 2012

dx.doi.org/10.1021/jp302465s | J. Phys. Chem. B 2012, 116, 11687−11694

specific conductivity (0.8−1.0) × 10^{-8} S cm^{-3} was obtained. The purity of the liquid was checked by measuring its density and viscosity which were in good agreement with the literature values[22,23] as shown in Table 1.

Table 1. Values of Density (ρ), Viscosity (η), and Relative Permittivity (ε_r) of ACN, THF, and 1,3-DO and Their Binary Mixtures[a]

	$\rho \times 10^{-3}$(kg m^{-3})		η (mPa s)		
solvents	expt	lit.	expt	lit.	ε_r
w_1 = 1.00	0.77668	0.77667[22]	0.344	0.3446[22]	35.95[38]
w_2 = 1.00	0.88074	0.88072[24]	0.463	0.4630[25]	7.58[38]
w_3 = 1.00	1.05873	1.05873[27]	0.589	0.5892[27]	7.31[38]
ACN(1) + THF(2)					
w_1 = 0.25	0.85473		0.433		14.67[b]
w_1 = 0.50	0.82871		0.404		21.77[b]
w_1 = 0.75	0.80269		0.374		28.86[b]
ACN(1) + 1,3-DO(3)					
w_1 = 0.25	0.98822		0.528		14.47[b]
w_1 = 0.50	0.91770		0.467		21.63[b]
w_1 = 0.75	0.84719		0.406		28.79[b]
THF(2) + 1,3-DO(3)					
w_2 = 0.25	1.01423		0.558		7.38[b]
w_2 = 0.50	0.96974		0.526		7.45[b]
w_2 = 0.75	0.92524		0.495		7.51[b]

[a] w_1, w_2, and w_3 are the mass fractions of ACN, THF, and 1,3-DO, respectively at T = 298.15 K. [b] Obtained by interpolation of literature data from ref 33.

Tetrahydrofuran (THF), Merck, India, was kept several days over potassium hydroxide (KOH), refluxed for 24 h, and distilled over lithium aluminum hydride ($LiAlH_4$) described earlier.[13] The purified solvent had a boiling point of 339 K and a specific conductance of 0.81 × 10^{-6} S cm^{-3}. The density and viscosity of the purified solvent were in good agreement with the literature data[24,25] as shown in Table 1. The purity of the solvent was ≥98.9%.

1,3-Dioxolane (1,3-DO) from Merck, containing 0.3% water and 0.005% peroxides and sterilized with butylated hydroxytoluene (BHT), was purified by heating under reflux with PbO_2 for 2 h, then cooled and filtered. After addition of xylene to the filtrate, the mixture was fractionally distilled.[26] The solvent obtained after purification had a boiling point of 348 K. The density and viscosity of the purified solvent were in good agreement with the literature[27] as shown in Table 1. The purity of the solvent finally obtained was ≥99.0%.

2.2. Apparatus and Procedure. All the binary solvent mixtures were prepared by mixing the required volume of ACN, THF, and 1,3-DO using the appropriate conversion of the required mass of each solvent into volume at 298.15 K using experimental densities.[28] For the preparation of the solvent mixtures, the required weighed amount of solvent was transferred to a volumetric flask and the flask was filled up to the mark. The stock solutions of the salt in binary solvent mixtures were prepared by mass (Mettler Toledo AG-285 with uncertainty ±0.0003 g). For conductance, the working solutions were obtained by mass dilution of the stock solutions. The densities of the solvents and solutions were measured with vibrating-tube density meter (Anton Paar, DMA 4500M), maintained at ±0.01 K of the desired temperature and calibrated at the experimental temperature with doubly distilled water and dry air. The uncertainty in density was estimated to be ±0.000 01 g cm^{-3}, and the viscosity was measured by means of a suspended Ubbelohde type viscometer, calibrated at 298.15 ± 0.01 K with doubly distilled water and purified methanol using density and viscosity values from the literature, and the efflux time of flow was recorded with a digital stopwatch correct to ±0.01 s. The uncertainty of the viscosity measurements was ±0.003 mPa s. The details of the methods and experimental techniques have been described elsewhere.[28,30]

The conductance measurements were carried out in a Systronics-308 conductivity bridge of accuracy ±0.01%, using a dip-type immersion conductivity cell, CD-10, having a cell constant of approximately 0.1 ± 0.001 cm^{-1}. Measurements were made in a thermostate water bath maintained at T = 298.15 ± 0.01 K. The cell was calibrated by the method proposed by Lind et al.,[31] and the cell constant was measured based on 0.01 M aqueous KCl solution.[32] During the conductance measurements, cell constant was maintained within the range 1.10−1.12 cm^{-1}. The conductance data were reported at a frequency of 1 kHz and the accuracy was ±0.3%. During all the measurements, uncertainty of temperatures was ±0.01 K.

The values of relative permittivity (ε_r) of the solvent mixtures were assumed to be an average of those of the pure liquids and calculated using the procedure as described by Rohdewald and Moldner.[33]

3. RESULTS AND DISCUSSION

3.1. Electrical Conductance. *3.1.1. Ion-Pair Formation.* The electrolyte was freely soluble in all proportions of the solvent/solvent mixtures. The physical properties of the pure and binary solvent mixtures in different mass fractions at 298.15 K are reported in Table 1, where appropriate corrections were made by the specific conductance of the solvents at that temperature.

The specific conductance (κ, μS cm^{-1}) of salt solutions under investigation with a molar concentration within the range of 1.05 × 10^{-5} to 1.42 × 10^{-2} M in different mass fractions (w = 0.00, 0.25, 0.50, 0.75, 1.00) were measured. The molar conductance (Λ) for all the systems studied was calculated using the following equation[34]

$$\Lambda = 1000\kappa/c \quad (1)$$

where c is the molar concentration and κ is the measured specific conductance of the studied solution. The molar conductances (Λ) of [Bu_4PBF_4] in different binary solvent mixtures were calculated at the corresponding molar concentrations (c) in solvent systems ACN + THF, ACN + 1,3-DO, and THF + 1,3-DO and given in Table 2. For the solvent and solvent mixtures as the range of higher to moderate relative permittivity (ε_r = 35.95 to 14.47), the conductance curves (Λ versus $\sqrt{c}$) were linear, depicted in Figure 1, and extrapolation of $\sqrt{c}$ = 0 evaluated the starting limiting molar conductance for the electrolytes; however, as the relative permittivity (ε_r) dropped to ε_r < 10 for pure THF (7.58), 1,3-DO (7.31), and their binary mixture, nonlinearity in Figure 2 was observed in conductance curves. Thus, the conductance data in ACN + THF and ACN + 1,3-DO solvent mixtures have been analyzed using the Fuoss conductance equation.[35,36] For a given set of conductivity values (c_j, Λ_j, j = 1,...,n) three adjustable parameters, the limiting molar conductance (Λ_o), the association constant (K_A), and the distance of closest approach of ions (R), are derived from the following set of equations.

$$\Lambda = P\Lambda_o[(1 + R_X) + E_L] \quad (2)$$

dx.doi.org/10.1021/jp302465s | J. Phys. Chem. B 2012, 116, 11687−11694

Table 2. Molar Conductance (Λ) and the Corresponding Concentration (c) of Bu_4PBF_4 in ACN, THF, and 1,3-DO and Their Binary Mixtures[a]

$c \times 10^4$ (mol dm^{-3})	$\Lambda \times 10^4$ (S m^2 mol^{-1})	$c \times 10^4$ (mol dm^{-3})	$\Lambda \times 10^4$ (S m^2 mol^{-1})	$c \times 10^4$ (mol dm^{-3})	$\Lambda \times 10^4$ (S m^2 mol^{-1})
acetonitrile		tetrahydrofuran		1,3-dioxolane	
9.32	167.16	0.25	27.73	0.11	19.95
17.09	165.08	0.38	24.18	0.21	16.50
23.66	163.92	0.55	20.96	0.30	14.08
29.29	162.75	0.70	18.54	0.39	12.25
34.18	162.07	0.90	16.27	0.46	10.75
42.22	160.81	1.01	15.08	0.57	9.42
48.57	160.00	1.16	13.71	0.69	8.62
55.93	158.89	1.34	12.65	0.83	8.23
63.10	158.13	1.48	12.15	0.94	9.52
70.49	157.26	1.66	12.06	1.03	10.99
77.52	156.45	1.91	13.03	1.12	13.41
82.98	155.90	2.16	15.48	1.20	15.65
		ACN(1) + THF(2)			
w_1 = 0.25		w_1 = 0.50		w_1 = 0.75	
27.01	81.80	19.57	109.89	13.63	137.12
36.30	79.80	28.81	107.06	22.35	134.91
47.16	77.75	37.21	105.07	29.98	132.90
58.07	75.80	47.75	103.04	39.11	130.92
67.75	74.81	56.65	101.35	46.40	129.87
76.67	73.41	64.12	100.31	54.82	128.41
88.57	72.26	70.46	99.50	60.77	127.81
97.17	71.15	78.78	98.07	68.66	126.46
103.98	70.25	86.34	96.91	76.00	125.35
112.17	69.10	93.74	95.96	81.43	124.46
118.59	68.40	103.53	95.00	88.93	123.75
125.73	68.02	109.94	94.05	94.38	123.14
		ACN(1) + 1,3-DO(3)			
w_1 = 0.25		w_1 = 0.50		w_1 = 0.75	
31.42	77.22	22.56	104.82	15.81	133.75
40.07	75.70	31.58	102.30	21.09	132.20
48.72	74.27	41.34	100.41	28.84	130.19
57.46	72.88	49.70	98.81	37.45	128.38
68.06	71.39	60.53	96.90	45.70	126.99
77.26	70.10	70.73	95.22	54.46	125.29
89.11	68.56	80.46	93.60	62.73	123.98
100.60	66.89	88.55	92.42	70.73	122.70
113.42	65.53	97.81	91.30	77.44	121.79
121.88	64.61	108.58	89.77	85.43	120.76
131.79	63.72	117.87	88.80	91.81	119.82
140.42	62.89	124.19	88.00	99.76	118.84
		THF(2) + 1,3-DO(3)			
w_2 = 0.25		w_2 = 0.50		w_2 = 0.75	
0.13	22.52	0.16	23.87	0.20	25.56
0.22	19.28	0.26	20.86	0.31	22.25
0.32	16.63	0.35	18.65	0.42	19.89
0.45	14.10	0.44	16.63	0.58	16.96
0.58	12.28	0.56	14.72	0.71	15.30
0.73	10.77	0.70	13.09	0.88	13.46
0.87	9.84	0.84	11.77	1.08	11.95
1.01	9.67	1.03	10.67	1.27	11.13
1.14	10.02	1.23	10.82	1.44	10.96
1.23	10.85	1.39	11.74	1.57	11.63
1.38	13.99	1.52	13.73	1.70	13.09
1.48	17.09	1.64	16.84	1.84	15.98

[a] w_1, w_2, and w_3 are the mass fractions of ACN, THF, and 1,3-DO, respectively, at T = 298.15 K.

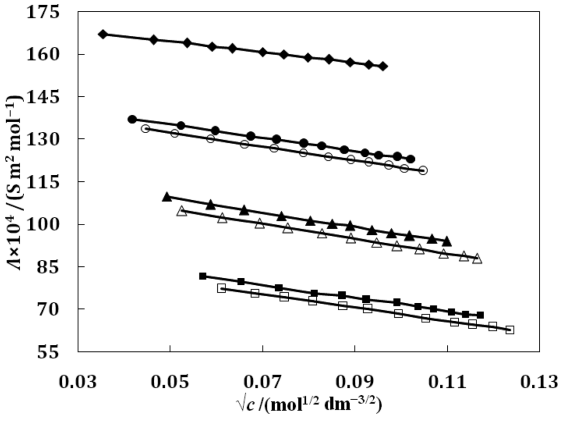

Figure 1. Plot of molar conductance (Λ) and the square root of concentration ($\sqrt{c}$) of Bu_4PBF_4 in w_1 = 0.25 (■), w_1 = 0.50 (▲), w_1 = 0.75 (●), and w_1 = 1.00 (◆) of ACN in THF and w_1 = 0.25 (□), w_1 = 0.50 (△), w_1 = 0.75 (○), and w_1 = 1.00 (◆) of ACN in 1,3-DO at T = 298.15 K.

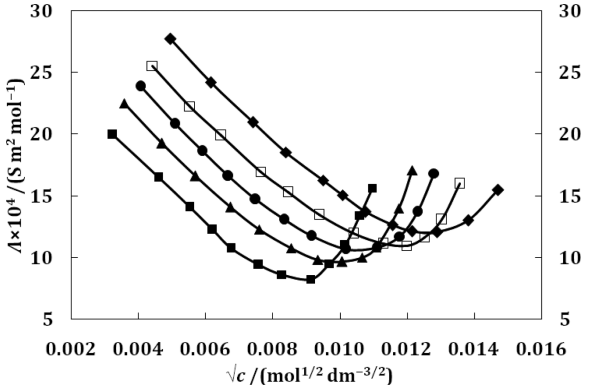

Figure 2. Plot of molar conductance (Λ) and the square root of concentration ($\sqrt{c}$) of Bu_4PBF_4 in w_2 = 0.00 (■), w_2 = 0.25 (▲), w_2 = 0.50 (●), w_2 = 0.75 (□), and w_2 = 1.00 (◆) of THF in 1,3-DO at T = 298.15 K.

$$P = 1 - \alpha(1 - \gamma) \tag{3}$$

$$\gamma = 1 - K_A c\gamma^2 f^2 \tag{4}$$

$$-\ln f = \beta\kappa/2(1 + \kappa R) \tag{5}$$

$$\beta = e^2/(\varepsilon_r k_B T) \tag{6}$$

$$K_A = K_R/(1 - \alpha) = K_R/(1 + K_S) \tag{7}$$

where R_X is the relaxation field effect, E_L is the electrophoretic countercurrent, k^{-1} is the radius of the ion atmosphere, ε_r is the relative permittivity of the solvent mixture, e is the electron charge, c is the molarity of the solution, k_B is the Boltzmann constant, K_A is the overall paring constant, K_S is the association constant of the contact pairs, K_R is the association constant of the solvent-separated pairs, γ is the fraction of solute present as unpaired ion, α is the fraction of contact pairs, f is the activity

dx.doi.org/10.1021/jp302465s | J. Phys. Chem. B 2012, 116, 11687−11694

Table 3. Limiting Molar Conductivity (Λ_o), Association Constant (K_A), Distance of Closest Approach of Ions (R), Standard Deviations δ of Experimental Λ from Eq 2, Walden Product ($\Lambda_o\eta$), and Free Energy Change ($\Delta G°$) of Bu_4PBF_4 in ACN and Its Binary Mixtures with THF and 1,3-DO[a]

solvent	$\Lambda_o \times 10^4$ (S m^2 mol^{-1})	$K_A \times 10^{-4}$ (dm^2 mol^{-1})	R (Å)	δ	$\Lambda_o\eta \times 10^4$ (S m^2 mol^{-1} mPa s)	$\Delta G°$ (kJ mol^{-1})
w_1 = 1.00	167.99	10.42	12.14	0.36	57.85	−2.86
ACN(1) + THF(2)						
w_1 = 0.25	87.88	30.65	12.10	0.22	38.09	−3.13
w_1 = 0.50	114.26	24.33	11.91	0.36	46.13	−3.07
w_1 = 0.75	139.56	16.59	11.76	0.38	52.21	−2.98
ACN(1) + 1,3-DO(3)						
w_1 = 0.25	88.95	34.09	11.89	0.24	44.86	−3.15
w_1 = 0.50	110.44	26.14	11.77	0.17	51.55	−3.09
w_1 = 0.75	136.93	18.04	11.69	0.32	55.54	−3.00

[a] w_1 are the mass fractions of ACN at T = 298.15 K.

coefficient, T is the absolute temperature, and β is twice the Bjerrum distance. The computations were performed using a program suggested by Fuoss. The initial Λ_o values for the iteration procedure were obtained from Shedlovsky extrapolation of the data. Input for the program is the set (c_j, Λ_j, j = 1,...,n), n, ε, η, T, initial values of Λ_o, and an instruction to cover a preselected range of R values.

The best value of a parameter is the one when equations are best fitted to the experimental data corresponding to minimum standard deviation δ for a sequence of predetermined R values, and standard deviation δ was calculated by the following equation

$$\delta^2 = \sum [\Lambda_j(\text{calcd}) - \Lambda_j(\text{obsd})]^2/(n - m) \quad (8)$$

where n is the number of experimental points and m is the number of fitting parameters. The conductance data were analyzed by fixing the distance of closest approach R with two parameter fit (m = 2). As for the electrolytes studied in various mass fractions (w_1 = 0.25, 0.50, 0.75, 1.00) of ACN, no significant minima were observed in the δ versus R curves, whereas the R values were arbitrarily preset at the center to center distance of solvent-separated ion pair.[21] Thus, R values are assumed to be

$$R = a + d \quad (9)$$

where $a = r_+ + r_-$ is the sum of the crystallographic radii of the cation (r_+) and anion (r_-) and d is the average distance corresponding to the side of a cell occupied by a solvent molecule. The distance d is given by[37]

$$d\ (\text{Å}) = 1.183(M/\rho)^{1/3} \quad (10)$$

where M is the molar mass of the solvent and ρ is its density. For mixed solvents, M is replaced by the mole fraction average molar mass (M_{av}) which is given by

$$M_{av} = M_1M_2/(w_1M_2 + w_2M_1) \quad (11)$$

where w_1 and w_2 are the mass fractions of the first and second component of molar mass M_1 and M_2, respectively. The values of Λ_o, K_A, and R obtained by this procedure are represented in Table 3. Perusal of Table 3 reveals that the limiting molar conductances (Λ_o) of the electrolytes decreases with the increase of content of ACN in the solvent mixture with THF and 1,3-DO. The table also reveals that the association of the [Bu_4PBF_4] is more in 1,3-DO than in THF and ACN, which is in the order 1,3-DO > THF > ACN, and its value decreases with increasing content of ACN in their binary mixtures. Hence the ion−solvent interaction increases with the increase in the amount of 1,3-DO and THF in their binary mixtures with ACN, leading to a lower conductance of [Bu_4PBF_4]. The lower viscosity of ACN also supports the above fact because with lower viscosity, the Λ_o value should increase. The fact is also in line with the increases of the relative permittivity (ε_r) of the solvents/solvent mixtures, although the decreasing trend of viscosity for the solvent mixtures with increasing content of ACN suggests concomitant increase in limiting molar conductances[37,39] for the electrolyte. The trend suggests solvent viscosity (η_o) is predominant over the relative permittivity (ε_r) in affecting the electrolytic conductance of the electrolyte under the studied media.

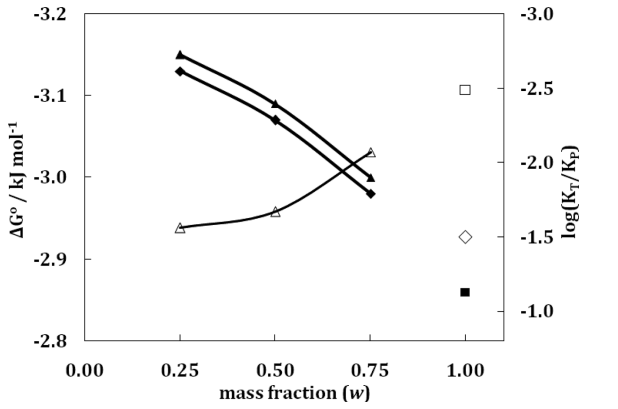

Figure 3. Plot of the free energy change ($\Delta G°$) vs mass fraction (w) of Bu_4PBF_4 in ACN (■), ACN + THF (◆), and ACN + 1,3-DO (▲), and log(K_T/K_P) vs mass fraction of Bu_4PBF_4 in THF (□), in 1,3-DO (◇), and in their binary mixture (△) at T = 298.15 K.

The trend in Λ_o values can be discussed through another characteristic function called the Walden product ($\Lambda_o\eta$), given in Table 3. The decreasing trend of the Walden product with decreasing amount of ACN in solvent mixture given in Table 3 and Figure 4 is in accordance with the concomitant increase of viscosity and decreasing limiting molar conductance of the electrolyte in the solvent/solvent mixtures. This is justified as the Walden product of an ion or solute is inversely proportional to the effective solvated radius (r_{eff}) of the ion or solute in a particular solvent/solvent mixture.[40]

$$\Lambda_o\eta = \frac{1}{6\Pi r_{eff}T} \quad (12)$$

This points out to the fact that the electrostatic ion−solvent interaction is strong in these cases. The variation of the Walden product reflects the change of solvation.[12,41] Though the

dx.doi.org/10.1021/jp302465s | J. Phys. Chem. B 2012, 116, 11687−11694

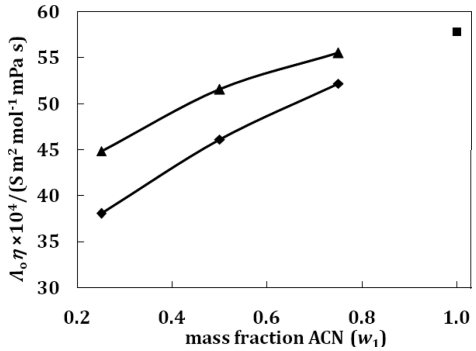

Figure 4. Plot of Walden product ($\Lambda_o\eta$) vs mass fraction of ACN (w_1) for Bu_4PBF_4 in ACN (■), ACN + THF (◆), and ACN + 1,3-DO (▲) at T = 298.15 K.

variation of the Walden product with solvent composition is difficult to interpret quantitatively, its variation with solvent composition can still be explained by preferential solvation[7,42] of the electrolyte by ACN, THF, and 1,3-DO molecules. At low concentration of ACN, the electrolytes are preferentially solvated in THF and 1,3-DO rather than by ACN.

The starting point for most evaluations of ionic conductance is Stokes' law which states that the limiting Walden product ($\lambda_o^{\pm}\eta$, the limiting ionic conductance−solvent viscosity product) for any singly charged spherical ion is a function only of the ionic radius and thus, under normal conditions, is a constant. The ionic conductances $\lambda_o^{\pm}$ (for the Bu_4P^+ cation and BF_4^- anion) in different solvent mixtures, mass fraction w_1 = 0.25, 0.50, 0.75, 1.00 of ACN with THF and 1,3-DO, were calculated using tetrabutylammonium tetraphenylborate (Bu_4NBPh_4) as a "reference electrolyte" following the scheme as suggested by B. Das et al.[43] We have calculated the ionic limiting molar conductances $\lambda_o^{\pm}$, in our solvent compositions by interpolation of conductance data from the literature[44] using cubic spline fitting. The $\lambda_o^{\pm}$ values were in turn utilized for the calculation of Stokes' radii (r_S) according to the classical expression[45]

$$r_S = \frac{F^2}{6\pi N_A \lambda_o^{\pm} r_c} \tag{13}$$

Ionic Walden products $\lambda_o^{\pm}\eta$, Stokes' radii r_S, and crystallographic radii r_c are presented in Table 4. The trends in Walden products $\Lambda_o\eta$ and ionic Walden products $\lambda_o^{\pm}\eta$ for the electrolytes in the solvents/solvent mixtures of ACN with THF and 1,3-DO are depicted in Tables 3 and 4 and Figures 4 and 5, respectively. It shows that both the ionic Walden products $\lambda_o^{\pm}\eta$ and Walden products $\Lambda_o\eta$ for the electrolyte increase almost linearly as the ACN content increases in the solvent mixtures. For Bu_4P^+ and BF_4^- ions, the Stokes' radii r_S are either lower or comparable to their crystallographic radii r_c, and this suggests that the ions are comparatively less solvated than alkali metal ions due to their intrinsic low surface charge density. The distance parameter R, shown in Table 3, is the least distance that two free ions can approach before they merge into ion pair. R values have been found to increase with increase in mass fraction of ACN (w_1) in the solvent mixture.

The nature of the curve for the Gibbs free energy changes for ion-pair formation, $\Delta G°$, clearly predicts the tendency for ion-pair formation. The Gibbs free energy change $\Delta G°$ is given by the following relationship[46] and is given in Table 3.

$$\Delta G° = -RT \ln K_A \tag{14}$$

Table 4. Limiting Ionic Conductance ($\lambda_o^{\pm}$), Ionic Walden Product ($\lambda_o^{\pm}\eta$), Stokes' Radii (r_S), and Crystallographic Radii (r_c)[a] of Bu_4PBF_4 in ACN and Its Binary Mixtures with THF and 1,3-DO[b]

solvents	ion	$\lambda_o^{\pm}$ (S m^2 mol^{-1})	$\lambda_o^{\pm}\eta$ (S m^2 mol^{-1} mPa s)	r_S (Å)	r_c (Å)
w_1 = 1.00	Bu_4P^+	64.86	22.34	3.67	4.42
	BF_4^-	103.12	35.52	2.31	2.78
ACN(1) + THF(2)					
w_1 = 0.25	Bu_4P^+	33.93	14.71	5.57	4.42
	BF_4^-	53.95	23.38	3.50	2.78
w_1 = 0.50	Bu_4P^+	44.12	17.81	4.60	4.42
	BF_4^-	70.15	28.32	2.89	2.78
w_1 = 0.75	Bu_4P^+	53.89	20.16	4.06	4.42
	BF_4^-	85.67	32.05	2.56	2.78
ACN(1) + 1,3-DO(3)					
w_1 = 0.25	Bu_4P^+	32.80	17.32	4.73	4.42
	BF_4^-	52.15	27.54	2.98	2.78
w_1 = 0.50	Bu_4P^+	42.64	19.91	4.12	4.42
	BF_4^-	67.80	31.65	2.59	2.78
w_1 = 0.75	Bu_4P^+	52.87	21.44	3.82	4.42
	BF_4^-	84.06	34.10	2.40	2.78

[a]Crystallographic radii of cation and anion from refs 52 and 53, respectively. [b]w_1 is the mass fraction of ACN at T = 298.15 K.

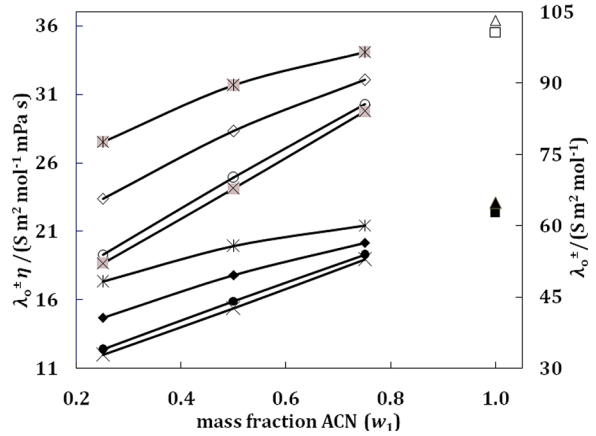

Figure 5. Plot of ionic Walden product ($\lambda_o^{\pm}\eta$) vs mass fraction (w) for Bu_4P^+ in ACN (■), ACN + THF (◆), and ACN + 1,3-DO (∗) and for BF_4^- in ACN (□), ACN + THF (◇), and ACN + 1,3-DO (∗). Plot of limiting ionic conductance ($\lambda_o^{\pm}$) vs mass fraction (w) for Bu_4P^+ in ACN (▲), ACN + THF (●), and ACN + 1,3-DO (×) and for BF_4^- in ACN (△), ACN + THF (○), and ACN + 1,3-DO (×), at T = 298.15 K.

The negative values of $\Delta G°$ can be explained by considering the participation of specific covalent interaction in the ion-association process. The increase in the value of $\Delta G°$ of [Bu_4PBF_4] with increasing amount of ACN in the solvent mixtures leads to the decrease in the ion−solvent interaction.

There are marked characteristic behaviors in the K_A values, which generally decrease as the quantity of ACN is increased in mixtures; the thermal motion probably destroys the solvent structure. However, ion association for the electrolyte increases as the concentration of THF and 1,3-DO increases in the mixtures.

The schematic representation of ion solvation, for the particular ion in the studied solvent mixtures (ACN + THF, ACN + 1,3-DO), in view of various derived parameters is depicted in Scheme 1, where w_1 is mass fraction of ACN.

dx.doi.org/10.1021/jp302465s | J. Phys. Chem. B 2012, 116, 11687−11694

Scheme 1

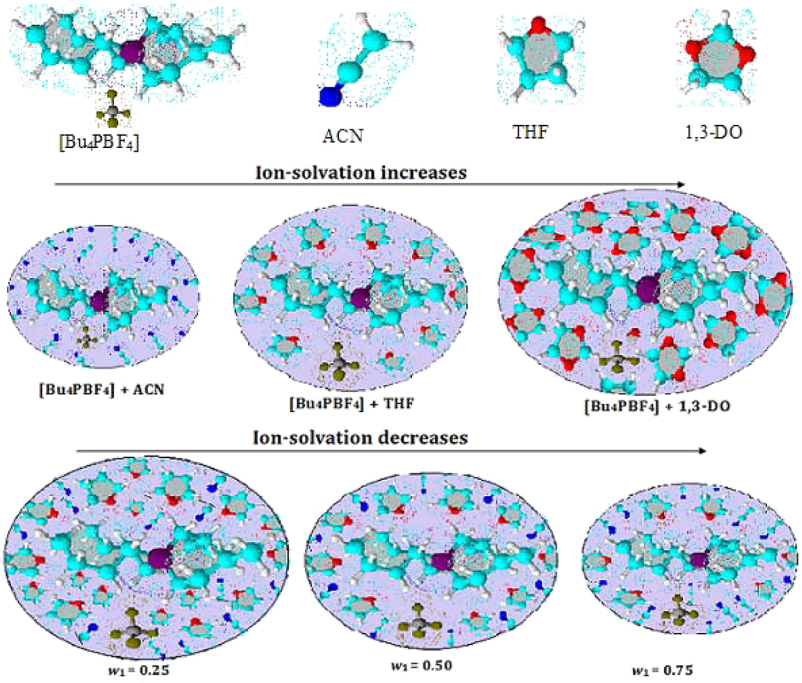

3.1.2. Triple-Ion Formation. Figure 2 presents the graphical representation of Λ versus $\sqrt{c}$ which shows that the salt follows the same trend, i.e., decreases with increasing concentration, reaches a minimum and then increases. Due to the deviation of the conductometric curves from linearity in the case of Bu_4PBF_4 in THF ($\varepsilon_r = 7.58$), 1,3-DO ($\varepsilon_r = 7.31$), and their binary mixtures, the conductance data have been analyzed by the classical Fuoss–Kraus theory of triple-ion formation in the form[37,46]

$$\Lambda g(c)\sqrt{c} = \frac{\Lambda_o}{\sqrt{K_P}} + \frac{\Lambda_o^T K_T}{\sqrt{K_P}}\left(1 - \frac{\Lambda}{\Lambda_o}\right)c \tag{15}$$

where the $g(c)$ is a factor that lumps together all the intrinsic interaction terms and is defined by

$$g(c) = \frac{\exp\{-2.303\beta'(c\Lambda)^{0.5}/\Lambda_o^{0.5}\}}{\{1 - S(c\Lambda)^{0.5}/\Lambda_o^{1.5}\}(1 - \Lambda/\Lambda_o)^{0.5}} \tag{16}$$

$$\beta' = 1.8247 \times 10^6/(\varepsilon T)^{1.5} \tag{17}$$

$$S = \alpha\Lambda_o + \beta = \frac{0.8204 \times 10^6}{(\varepsilon T)^{1.5}}\Lambda_o + \frac{82.501}{\eta(\varepsilon T)^{0.5}} \tag{18}$$

In the above equations, Λ_o is the sum of the molar conductance of the simple ions at infinite dilution, Λ_o^T is the sum of the conductance value of the two triple ions $[(Bu_4P)_2]^+BF_4$ and $Bu_4P[(BF_4)_2]^-$ for Bu_4PBF_4 salt; $K_P \approx K_A$ and K_T are the ion-pair and triple-ion formation constants, respectively, and S is the limiting Onsager coefficient. To make eq 15 applicable, the symmetrical approximation of the two possible formation constants of triple ions, $K_{T1} = [(Bu_4P)_2]^+BF_4/\{[Bu_4P^+][Bu_4PBF_4]\}$ and $K_{T2} = Bu_4P[(BF_4)_2]^-/\{[BF_4^-][Bu_4PBF_4]\}$, equal to each other have been adopted, i.e., $K_{T1} = K_{T2} = K_T$[47] and Λ_o values for the studied electrolyte have been calculated following the scheme as suggested by Krumgalz.[48] The calculated values are listed in Table 5. Λ_o^T has been calculated by setting the triple-ion conductance equal to $(2/3)\Lambda_o$.[49]

Table 5. Calculated Limiting Molar Conductance of Ion Pair (Λ_o), Limiting Molar Conductance of Triple Ion (Λ_o^T), and Slope and Intercept of Eq 15 of Bu_4PBF_4 in THF, 1,3-DO, and Their Binary Mixture[a]

solvents	$\Lambda_o \times 10^4$ (S m^2 mol^{-1})	$\Lambda_o^T \times 10^4$ (S m^2 mol^{-1})	slope $\times 10^{-2}$	intercept
$w_2 = 1.00$	74.93	49.98	0.82	0.15
$w_3 = 1.00$	43.85	29.25	6.19	0.07
THF(2) + 1,3-DO(3)				
$w_2 = 0.25$	46.98	31.34	4.64	0.09
$w_2 = 0.50$	52.78	35.20	3.81	0.10
$w_2 = 0.75$	61.36	40.93	1.70	0.12

[a] w_2 and w_3 are mass fractions of THF and 1,3-DO at $T = 298.15$ K.

The ratio Λ_o^T/Λ_o was thus set equal to 0.667 during linear regression analysis of eq 15. Table 5 shows the calculated limiting molar conductance of simple ion (Λ_o), limiting molar conductance of triple ion (Λ_o^T), and slope and intercept of eq 15 for Bu_4PBF_4 in THF, 1,3-DO, and their binary mixture at 298.15 K. The linear regression analysis of eq 15 for the electrolytes with an average regression constant, $R^2 = 0.9653$ gives intercepts and slopes. These values permit the calculation of other derived parameters such as K_P and K_T listed in Table 6. A perusal of Table 5 shows that the major portion of the electrolytes exists as ion pairs with a minor portion as triple ions. The tendency of triple ion formation can be judged from the K_T/K_P ratios and $\log(K_T/K_P)$, which are highest in 1,3-DO. These ratios suggest that strong association between the ions is due to the Coulombic interactions as well as to covalent forces in the solution. These results are in good agreement with those of Hazra et al.[50] At very low permittivity of the solvent, i.e., $\varepsilon < 10$, electrostatic ionic interactions are very large. So the ion pairs attract the free cations or anions present in the solution medium as the distance of the closest approach of the ions becomes minimum. This results in the formation of triple ions,

dx.doi.org/10.1021/jp302465s | J. Phys. Chem. B 2012, 116, 11687–11694

Table 6. Salt Concentration at the Minimum Conductivity (c_{min}) along with the Ion Pair Formation Constant (K_P) and Triple Ion Formation Constant (K_T) of Bu_4PBF_4 in THF, 1,3-DO, and Their Binary Mixture[a]

solvent/solvent mixture	$c_{min} \times 10^4$ (mol dm^{-3})	log c_{min}	$K_P \times 10^{-4}$ (mol m^{-3})$^{-1}$	$K_T \times 10^{-3}$ (mol m^{-3})$^{-1}$	$(K_T/K_P) \times 10^3$	log(K_T/K_P)
w_2 = 1.00	1.66	−3.78	25.36	0.83	3.27	−2.49
w_3 = 1.00	0.83	−4.08	45.35	14.26	31.43	−1.50
THF(2) + 1,3-DO(3)						
w_2 = 0.25	1.01	−3.99	28.99	7.98	27.53	−1.56
w_2 = 0.50	1.03	−3.98	25.76	5.49	21.32	−1.67
w_2 = 0.75	1.44	−3.84	23.92	2.03	8.50	−2.07

[a] w_2 and w_3 are mass fractions of THF and 1,3-DO at T = 298.15 K.

Scheme 2

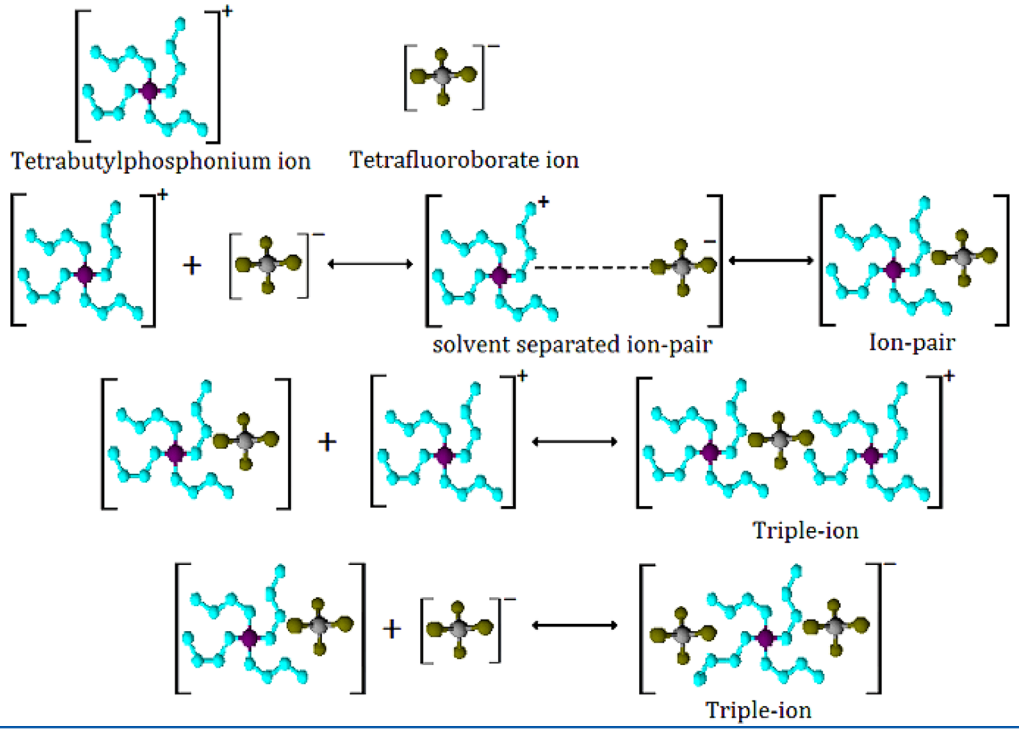

which acquires the charge of the respective ions, attracted from the solution bulk;[44,46] i.e.

$$M^+ + A^- \leftrightarrow M^+ \cdots A^- \leftrightarrow MA \quad \text{(ion pair)} \tag{19}$$

$$MA + M^+ \leftrightarrow MAM^+ \quad \text{(triple ion)} \tag{20}$$

$$MA + A^- \leftrightarrow MAA^- \quad \text{(triple ion)} \tag{21}$$

where M^+ and A^- are Bu_4P^+ and BF_4^-, respectively. The effect of ternary association[41] thus removes some nonconducting species, MA, from solution, and replaces them with triple ions which increase the conductance manifested by nonlinearity observed in conductance curves for the electrolyte in THF, 1,3-DO and their binary mixtures. Scheme 2 depicts the pictorial representation of triple-ion formations for the electrolyte, as an example in THF + 1,3-DO binaries.

Furthermore, the ion-pair and triple-ion concentrations, C_P and C_T, respectively, of the [Bu_4PBF_4] in THF, 1,3-DO and their binary mixture have also been calculated using the following equations[51]

$$\alpha = 1/(K_P^{1/2}C^{1/2}) \tag{22}$$

$$\alpha_T = (K_T/K_P^{1/2})C^{1/2} \tag{23}$$

Table 7. Salt Concentration (c_{min}) at the Minimum Conductivity (Λ_{min}), the Ion-Pair Fraction (α), Triple-Ion Fraction (α_T), Ion-Pair Concentration (C_P), and Triple-Ion Concentration (C_T) of Bu_4PBF_4 in THF, 1,3-DO, and Their Binary Mixture[a]

solvent/solvent mixture	$c_{min} \times 10^4$ (mol dm^{-3})	$\Lambda_{min} \times 10^4$	α	α_T	$C_P \times 10^5$ (mol dm^{-3})	$C_T \times 10^6$ (mol dm^{-3})
w_2 = 1.00	1.66	12.06	0.153	0.021	15.14	3.54
w_3 = 1.00	0.83	8.23	0.162	0.193	11.78	16.06
THF(2) + 1,3-DO(3)						
w_2 = 0.25	1.01	9.67	0.184	0.149	12.77	15.09
w_2 = 0.50	1.03	10.67	0.193	0.110	11.75	11.38
w_2 = 0.75	1.44	10.96	0.170	0.049	14.04	7.15

[a] w_2 and w_3 are mass fractions of THF and 1,3-DO at T = 298.15 K.

$$C_P = C(1 - \alpha - 3\alpha_T) \tag{24}$$

$$C_T = (K_T/K_P^{1/2})C^{3/2} \tag{25}$$

Here, α and α_T are the fraction of ion pairs and triple ions present in the salt solutions and are given in Table 7. Thus, the values of C_P and C_T given in Table 7 indicate that the ions are mainly present as ion pairs even at high concentration, and a small fraction exist as triple ions. It is also observed that the

dx.doi.org/10.1021/jp302465s | J. Phys. Chem. B 2012, 116, 11687−11694

fraction of the triple ions in the solution increases with the increasing concentration in the studied mixed solvent media.

4. CONCLUSIONS

The present work reveals an extensive study on the ion-solvation behavior of the tetrabutylphosphonium tetrafluoroborate [Bu_4PBF_4] in ACN + THF, ACN + 1,3-DO, and THF + 1,3-DO mixtures through the conductometric measurements. It becomes clear that the electrolyte exists as ion pairs for the former two cases and as triple ions for the latter one. The tendency of the ion-pair and triple-ion formation depends on the size and the charge distribution of the ions. The effective size of the electrolyte increases in THF, 1,3-DO, and their binary mixtures due to preferential solvation in such a way that the sizes of the solvated ions follow their crystallographic radii. The degree of ion−solvent interaction also indicates that the salt prefers cyclic ether THF and 1,3-DO than ACN in their solvation or coordination sphere.

AUTHOR INFORMATION

Corresponding Author

*E-mail: mahendraroy2002@yahoo.co.in. Tel: +91-353-2776381. Fax: +91 353 2699001.

Notes

The authors declare no competing financial interest.

ACKNOWLEDGMENTS

The authors are thankful to the Departmental Special Assistance Scheme under the University Grants Commission, New Delhi (No.540/6/DRS/2007, SAP-1), India, and Department of Chemistry, University of North Bengal, for financial support and instrument facilities in order to continue this research work.

REFERENCES

(1) Welton, T. *Chem. Rev.* **1999**, *99*, 2071−2084.
(2) Earle, M. J.; Seddon, K. R. *Pure Appl. Chem.* **2000**, *72*, 1391−1398.
(3) Dupont, J.; de Souza, R. F.; Suarez, P. A. Z. *Chem. Rev.* **2002**, *102*, 3667−3692.
(4) Plechkova, N. V.; Seddon, K. R. *Chem. Soc. Rev.* **2008**, *37*, 123−150.
(5) Endres, F.; Zein El Abedin, S. *Phys. Chem. Chem. Phys.* **2006**, *8*, 2101−2116.
(6) Wang, P.; Zakeeruddin, S. M.; Moser, J. E.; Grätzel, M. *J. Phys. Chem. B* **2003**, *107*, 13280−13285.
(7) Janz, C. G.; Tomkins, R. P. T. *Non-aqueous Electrolytes Handbook*; Academic Press: New York, 1973; Vol. 2.
(8) Aurbach, D. *Non-aqueous Electrochemistry*; Marcel Dekker, Inc: New York, 1999.
(9) Krom, J. A.; Petty, J. T.; Streitwieser, A. *J. Am. Chem. Soc.* **1993**, *115*, 8024−8030.
(10) Das, D.; Das, B.; Hazra, D. K. *J. Solution Chem.* **2002**, *31*, 425−431.
(11) Guha, C.; Chakraborty, J. M.; Karanjai, S.; Das, B. *J. Phys. Chem. B* **2003**, *107*, 12814−12819.
(12) Das, D.; Das, B.; Hazra, D. K. *J. Solution Chem.* **2003**, *32*, 77−83.
(13) Roy, M. N.; Nandi, D.; Hazra, D. K. *J. Indian Chem. Soc.* **1993**, *70*, 123−126.
(14) Popvych, O. Tomkins, R. P. T. *Nonaqueous Solution Chemistry*; Wiley-Interscience: New York, 1981; Chapter 4.
(15) Matheson, A. J. *Molecular Acoustics*; Wiley-Interscience: London, 1971.
(16) Das, B.; Saha, N. *J. Chem. Eng. Data* **2000**, *44*, 2−5.
(17) Roy, M. N.; Pradhan, P.; Das, R. K.; Guha, P. G.; Sinha, B. *J. Chem. Eng. Data* **2008**, *53*, 1417−1420.
(18) Chanda, R.; Roy, M. N. *Fluid Phase Equilib.* **2008**, *269*, 134−138.
(19) Chen, Z.; Hojo, M. *J. Phys. Chem. B* **1997**, *101*, 10896−10902.
(20) Parvatalu, D.; Srivastava, A. K. *J. Chem. Eng. Data* **2003**, *48*, 608−611.
(21) Roy, M. N.; Sinha, B.; Dakua, V. K.; Sinha, A. *Pak. J. Sci. Ind. Res.* **2006**, *49*, 153−159.
(22) Saha, N.; Das, B. *J. Chem. Eng. Data* **1997**, *42*, 227−229.
(23) Prolongo, M. G.; Masegosa, R. M.; Fuentes, I. H.; Horta, A. *J. Phys. Chem.* **1984**, *88*, 2163−2167.
(24) Roy, M. N.; Dey, R.; Jha, A. *J. Chem. Eng. Data* **2001**, *46*, 1327−1329.
(25) Sinha, A.; Roy, M. N. *Phys. Chem. Liq.* **2006**, *44*, 303−314.
(26) Roy, M. N.; Sinha, A. *Fluid Phase Equilib.* **2006**, *243*, 133−141.
(27) Roy, M. N.; Ekka, D.; Dewan, R. *Fluid Phase Equilib.* **2012**, *314*, 113−120.
(28) Roy, M. N.; Dewan, R.; Sarkar, L. *J. Chem. Eng. Data* **2010**, *55*, 1347−1353.
(29) Sinha, B.; Sarkar, B. K.; Roy, M. N. *J. Chem. Thermodyn.* **2008**, *40*, 394−400.
(30) Bhattacharjee, A.; Roy, M. N. *Phys. Chem. Chem. Phys.* **2010**, *12*, 14534−14542.
(31) Lind, J. E., Jr.; Zwolenik, J. J.; Fuoss, R. M. *J. Am. Chem. Soc.* **1959**, *81*, 1557−1559.
(32) Roy, M. N.; Banerjee, A.; Das, R. K. *J. Chem. Thermodyn.* **2009**, *41*, 1187−1192.
(33) Rohdewald, P.; Moldner, M. *J. Phys. Chem.* **1973**, *77*, 373−377.
(34) El-Dossoki, F. I. *J. Mol. Liq.* **2010**, *151*, 1−8.
(35) Fuoss, R. M. *Proc. Natl. Acad. Sci. U.S.A.* **1978**, *75*, 16−20.
(36) Fuoss, R. M. *J. Phys. Chem.* **1978**, *82*, 2427−2440.
(37) Fuoss, R. M.; Accascina, F. *Electrolytic Conductance*; Interscience: New York, 1959.
(38) Covington, A. K.; Dickinson, T. *Physical chemistry of organic solvent systems*; Plenum: New York, 1973.
(39) Bockris, J. O.; Reddy, A. N. *Modern Electrochemistry*, 2nd ed.; Plenum Press: New York, 1998; p 552.
(40) Bhat, J. I.; Bindu, P. *J. Ind. Chem. Soc* **1995**, *72*, 783−790.
(41) Sinha, A.; Roy, M. N. *Phys. Chem. Liq.* **2007**, *45*, 67−77.
(42) Inove, N.; Xu, M.; Petrucci, S. *J. Phys. Chem.* **1987**, *91*, 4628−4635.
(43) Chakraborty, J. M.; Das, B. *Z. Phys. Chem.* **2004**, *218*, 219−230.
(44) Fuoss, R. M.; Hirsch, E. *J. Am. Chem. Soc.* **1960**, *82*, 1013−1017.
(45) Robinson, R. A.; Stokes, R. H. *Electrolyte Solutions*; Butterworth: London, 1959; Chapter 6, p 130.
(46) Fuoss, R. M.; Kraus, C. A. *J. Am. Chem. Soc.* **1933**, *55*, 2387−2399.
(47) Harada, Y.; Salamon, M.; Petrucci, S. *J. Phys. Chem.* **1985**, *89*, 2006−2010.
(48) Krumgalz, B. S. *J. Chem. Soc., Faraday Trans. 1* **1983**, *79*, 571−587.
(49) Delsignore, M.; Farber, H. *J. Phys. Chem.* **1985**, *89*, 4968−4973.
(50) Nandi, D.; Roy, M. N.; Hazra, D. K. *J. Indian Chem. Soc.* **1993**, *70*, 305.
(51) Nandi, D.; Das, S.; Hazra, D. K. *Ind. J. Chem. A* **1988**, *27*, 574−580.
(52) Philip, P. R.; Jolicoeur, C. *J. Phy. Chem* **1973**, *77*, 3071−3077.
(53) Libus, W.; Chachulski, B.; Fraczyk, L. *J. Solution Chem.* **1980**, *9* (5), 355−369.